

Article

The Application of Passive Radiative Cooling in Greenhouses

Chia-Hsin Liu ¹, Chyung Ay ², Chun-Yu Tsai ³ and Maw-Tien Lee ^{1,*}

¹ Department of Applied Chemistry, National Chia Yi University, Chiayi 60004, Taiwan; s1060301@mail.ncyu.edu.tw

² Department of Biomechatronic Engineering, National Chia Yi University, Chiayi 60004, Taiwan; cay@mail.ncyu.edu.tw

³ Program of Agriculture Science, National Chiayi University, Chiayi 60004, Taiwan; s1050005@mail.ncyu.edu.tw

* Correspondence: mtleee@mail.ncyu.edu.tw; Tel.: +886-5-2717691

Received: 31 October 2019; Accepted: 24 November 2019; Published: 27 November 2019



Abstract: At present, greenhouses are used to grow a variety of crops around the world. However, with the change of climate, the increasingly harsh weather makes it more and more disadvantageous for people to work inside, and plants are difficult to grow. Previous research has illustrated that radiative cooling can be realized by using certain nonmetal oxide particles created for emission in an infrared atmospheric transparency window, which is an environmentally friendly cooling method due to reducing energy consumption. Polyethylene (PE)-based formulations with a UV stabilizer and nonmetal oxide particles (NOP) were first granulated and then formed a monolayer film by co-injection molding. The experimental results show that due to passive radiative cooling, under the environmental conditions of 35 °C, and only considering the natural convection heat transfer, the net cooling power of the greenhouse film developed in this study is 28 W·m⁻² higher than that of the conventional PE film. The temperature inside the simulated greenhouse clad with the new greenhouse covering was on average 2.2 °C less than that of the greenhouse with the conventional PE film.

Keywords: covering material; passive cooling; infrared atmospheric transparency window

1. Introduction

Because of the change of climate, the temperature on the Earth's surface has risen, resulting in humans using a lot of energy to cool down, but the energy on the Earth is not inexhaustible, and concerns about the environment and energy conservation have become important issues worldwide [1,2]. Most of the cooling methods employed in the past have always required energy or resources to assist the heat dissipation, while radiative cooling is a natural cooling method on the Earth, which radiates heat to outer space through a transparency window in the atmosphere that is between 8 and 13 micrometers [3–26]. It refers to the process of dissipating the heat of objects to the space of the universe, having a lower temperature via thermal radiation. It is environmentally friendly and a potential way to make up for the problems caused by global warming during recent years, because this method offers an important impact regarding energy saving, for its ability to conduct without external energy.

Radiative cooling is a natural phenomenon on the Earth's surface. When the sunlight shines on the Earth's surface, it will be absorbed by the territory, and most of the thermal radiation can transmit through the atmospheric window, where it is highly transparent. It is astonishing that the spectrum of the atmospheric window is consistent with the range of wavelengths of thermal radiation from ground objects, which is a good illustration of how the Earth maintains its heat balance throughout the year.

From the mid-20th century, radiative cooling during nighttime through bulk materials comprising inherent infrared emissions has been widely studied and has been applied to rooftop cooling [3–6], but the peak cooling requirement occurs during the daytime. Daytime radiative cooling is difficult to achieve because of solar radiation. According to the nature of being, such as the Saharan silver ant's body and the cocoon made by wild silk moths, they have nanostructure biomaterials that inspire the progress of daytime radiative cooling materials. Firstly, Rephaeli et al. [7] present a metal-dielectric photonic structure, which achieved a net cooling power in excess of $100 \text{ W}\cdot\text{m}^{-2}$. Raman et al. [10] proposed a photonic radiative cooler and it achieved $4.9 \text{ }^\circ\text{C}$ below the ambient temperature under direct sunlight, with a cooling power of $40.1 \text{ W}\cdot\text{m}^{-2}$. Gentle and Smith first used a mixture of SiC and SiO_2 nanoparticles to yield high-performance cooling at a low cost [15], and then they proposed a stack of alternating layers of polymers [22]. This device also performed better than a commercial cool roof in reducing the temperature. Then, a nano-/microstructure, such as the plasmonic structures and metallic/nonmetal photonic crystals, was proposed in order to improve the challenge of using bulk materials and planar photonic devices during the daytime [7,16]. However, these radiators are challenging for practical realization so polymeric photonics and metamaterial were developed to make the radiative cooling device economic and scalable [11–13]. Yao Zhai et al. [12] manufactured a metamaterial composed randomly of silicon dioxide microspheres and backed by a silver layer. The metamaterial is extremely emissive across the atmospheric window due to the existence of strong phonon–polariton resonances of the embedded microspheres so it showed a radiative cooling power of $93 \text{ W}\cdot\text{m}^{-2}$ at noon under direct sunshine. Jun-long Kou et al. [13] used a polymer–silica mirror consisting of a fused silica wafer, coated with a polymer top layer and a silver back reflector, which achieved $8.2 \text{ }^\circ\text{C}$ under daytime, and it had a net cooling power of about $127 \text{ W}\cdot\text{m}^{-2}$ at an ambient temperature of 300 K under AM 1.5 solar irradiation. No matter what kinds of devices were used for radiative cooling in the past, they required identical features of a strong thermal emission and high solar reflection.

A greenhouse is an artificial building that shelters crops from harsh weather conditions. Solar radiation involves ultraviolet radiation (UV, 100–400 nm), visible radiation (VIS, 400–780 nm), and near-infrared radiation (NIR, 750–2500 nm) and penetrates into the greenhouse through the cladding to assist the crops in growing [27]. Among them, UV radiation affects film degradation and pollinator behavior, and NIR radiation is a direct source of heat. With the greenhouse effect being aggravated, the excessively high temperature makes it unfavorable for people to work inside the greenhouse and plants are hard to grow inside them.

In the literature [27–38], some active and passive cooling methods have been proposed in order to adjust the temperature inside the greenhouse. Active cooling, such as pad-fan systems, evaporative cooling systems, and heat pumps, may consume some energies and water resources. Passive cooling involves natural ventilation, shading, a liquid radiation filter (LRF), painting, and the NIR reflection additives. These methods have some limits, such as a high cost, being poisonous, and limited cooling effects. The infrared atmospheric window fits with the peak of thermal radiation wavelengths on general ambient temperatures [20], so, if the materials can emit the wavelength between 8–13 micrometers, the heat would be carried away to outer space by radiation, and this is a passive cooling. Based on this idea, connecting greenhouse covering materials with radiative cooling in order to save energy, CO_2 emission reduction, and, simultaneously, to adjust the temperature inside the greenhouse is a subject worthwhile to explore.

The most different to the devices used for the radiative cooling and those used in the greenhouse is high solar reflection. The greenhouse covering needs sunlight penetrating inside to keep the plants growing; therefore, it requires high transmittance in the visible radiation and high emissivity over the infrared atmosphere window. From past research, radiative cooling can be achieved by using some nonmetal oxide particle [7,10,12–17]. Unlike the devices mentioned above, the covering of a greenhouse needs neither high reflection nor a complicated device so we only added nonmetal oxide particles as the base of films for radiation cooling rather than using complex composition.

UV degradation of polymers is a well-known phenomenon, so a light stabilizer was added into the covering in this study to delay the aging of films. Nonmetal oxide particles were added to a polyethylene matrix, which was based on polyethylene (PE) and hindered amine light stabilizers, so as to fabricate the new greenhouse covering. The nonmetal oxide particles were prospective to improve the thermal radiation capability of the films in order to aid the new greenhouse covering in decreasing the temperatures inside the greenhouse primarily by passive cooling.

2. Materials and Methods

2.1. Materials and Preparing Plastic Films

The materials used in the experiment were polyethylene (PE; USI Corporation, Kaohsiung, Taiwan), nonmetal oxide (Taipei, Taiwan), and hindered amine light stabilizers (HALS; UV944, Lai Wai Co., Ltd., Taipei, Taiwan).

In order to get films that were uniformly dispersed, the mixtures were placed in a twin-screw kneading granulation/stretching apparatus to first be granulated. After the HALS (30 g) and PE (3000 g) were granulated, a sample was put into a co-injection molding apparatus, and then heated to 265 °C in order to produce the following films: PE@ with a thickness of 0.16–0.18 mm.

Nonmetal oxide particles (30 g), PE (3000 g), and HALS (30 g) were granulated. Next, the mixtures were placed in a co-injection molding apparatus, to be heated to 265 °C. Finally, monolayer films and the new greenhouse covering (PE@1.0S with a thickness of 0.16–0.18 mm) were produced.

2.2. Characterization of Prepared Plastic Films

We characterized the spectroscopic performance of PE, PE@, and PE@1.0S in infrared (4 to 20 μm) using Fourier-transform infrared spectroscopy (FTIR; SHIMADZU, 8400, Kyoto, Japan). The films were used as the covering to construct a simulated greenhouse. The temperatures of the simulated greenhouse were recorded in real time with thermocouples (TECPEL Co., LTD., DTM-319A, New Taipei, Taiwan). Three thermocouples were placed on the film (surface temperature) in the greenhouse, in the middle of the greenhouse (internal temperature), and outside the greenhouse (ambient temperature) individually. The distance between the two greenhouses was 15–20 cm. When measuring temperature, we placed a mat at the bottom of the greenhouse to block the heat from the ground to reduce the effect on temperature measurements. The observed temperatures were used for evaluating the cooling performance of the new greenhouse covering.

2.3. Energy Balance of a Radiative Cooling Structure

On the whole, the light on an object may be divided into absorbed, reflected, or transmitted. The absorption (α), reflection (ρ), and transmission (τ) of an object are defined as $\alpha + \rho + \tau = 1$. [20]. For a greenhouse facing clear sky as shown in Figure 1, the net cooling power P_{net} of the surface is described as follows:

$$P_{net}(T_s, T_a) = P_{rad}(T_s) - P_{atm}(T_a) - P_{solar} - P_c \quad (1)$$

where T_s is the surface temperature, T_a is the ambient temperature, P_{rad} is the thermal emission power radiated out by the substance, P_{atm} is the absorbed atmospheric irradiation at a temperature T_a , P_{solar} is the incident solar power absorbed by the structure, and P_c is the nonradiative (i.e., conductive + convective) heat transfer.

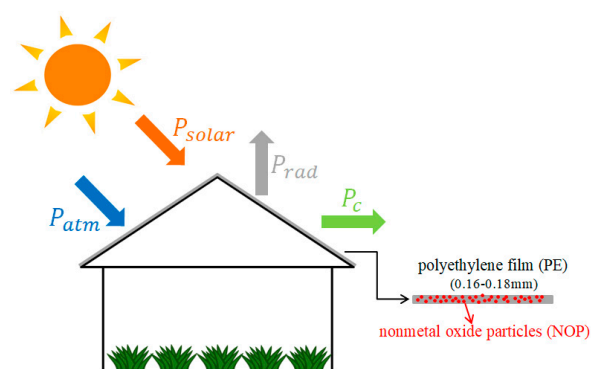


Figure 1. A schematic indicating the heat fluxes for a greenhouse.

3. Results

3.1. FTIR Spectrum of the Samples

Figure 2 is an FTIR spectrum between 500 and 2500 cm^{-1} (4 to $20\text{ }\mu\text{m}$) of different covering films. When PE added HALS (PE@), a significant peak appeared at 1575 cm^{-1} , and this peak was attributed to the characteristic absorption of the conjugated $\text{C}=\text{N}$ in the HALS. A characteristic peak near 1000 cm^{-1} emerged significantly after adding nonmetal oxide particles (PE@1.0S), and it corresponded to nonmetal oxide. The absorption peak at 720 , 1380 , and 1460 cm^{-1} belonged to $-\text{CH}_2-$ in linear low-density polyethylene.

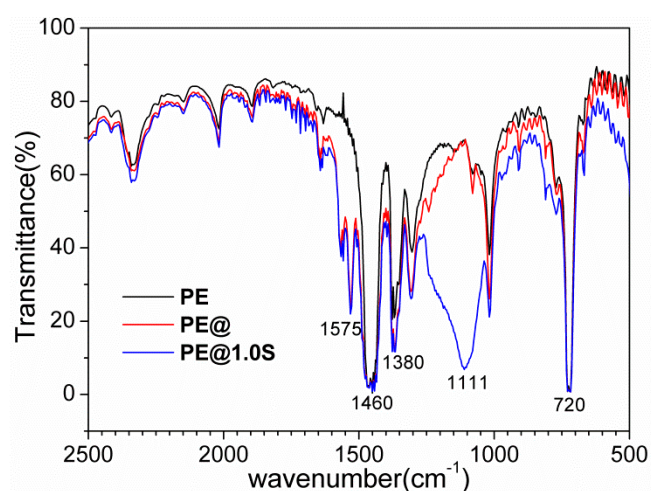


Figure 2. Fourier-transform infrared spectroscopy (FTIR) spectra of different films. PE—polyethylene; PE@—PE with added hindered amine light stabilizers (HALS); PE@1.0S—PE@ with added nonmetal oxide particles.

3.2. Cooling Performance

We built a simple small simulated greenhouse ($32 \times 20 \times 25\text{ cm}$; Figure 3) and measured the temperature on the covering to observe the cooling performance of PE@1.0S, as well as the ambient temperature from 11:00 to 13:00 in Chiayi, Taiwan, as shown in Figure 4. We used PE as a comparison, and under nearly $35\text{ }^\circ\text{C}$ ambient conditions, the average temperature on the PE covering and PE@1.0S was $52.01\text{ }^\circ\text{C}$ and $49.69\text{ }^\circ\text{C}$, respectively. Although these experiments were conducted on a sunny day and in a space surrounded by narrow buildings, occasionally some clouds appeared, causing occasional drops in temperature.



Figure 3. A simple simulated greenhouse.

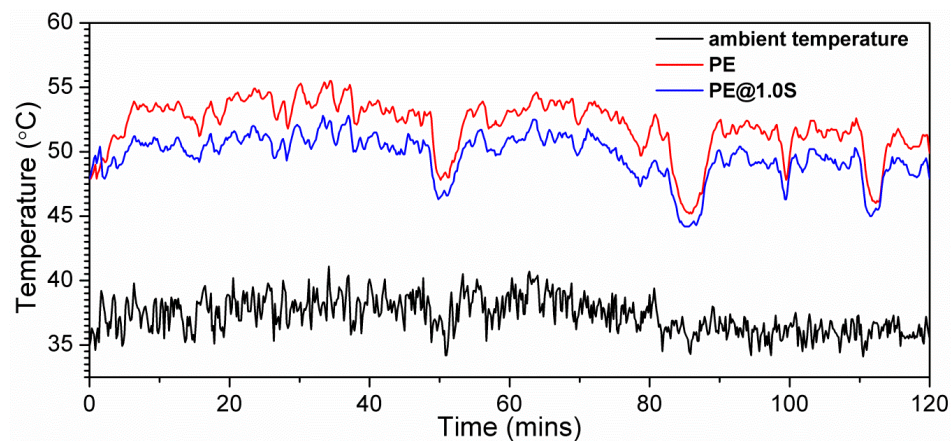


Figure 4. The temperature trend of PE and PE@1.0S on the surface of the covering and the ambient temperature.

As shown in Figure 5, we also measured the temperature inside the greenhouse and the ambient temperature at the same time from 11:00 to 13:00 in Chiayi, Taiwan, and occasionally some clouds appeared, which resulted in the abrupt dips in the temperature trend. Using PE as a comparison, the air temperature inside the greenhouse had a maximum temperature variance of 5.1 °C, and an average variance of 2.2 °C under nearly 35 °C ambient conditions. This result illustrated that PE@1.0S possessed a good cooling performance and it attributed to passive cooling, resulting from emitting thermal radiation in the atmosphere window by the property of nonmetal oxide particles. The addition of the nonmetal oxide particles was valid in lowering the temperature inside the greenhouse and it can be proved by the value of the cooling heat flux, calculated in the following sections.

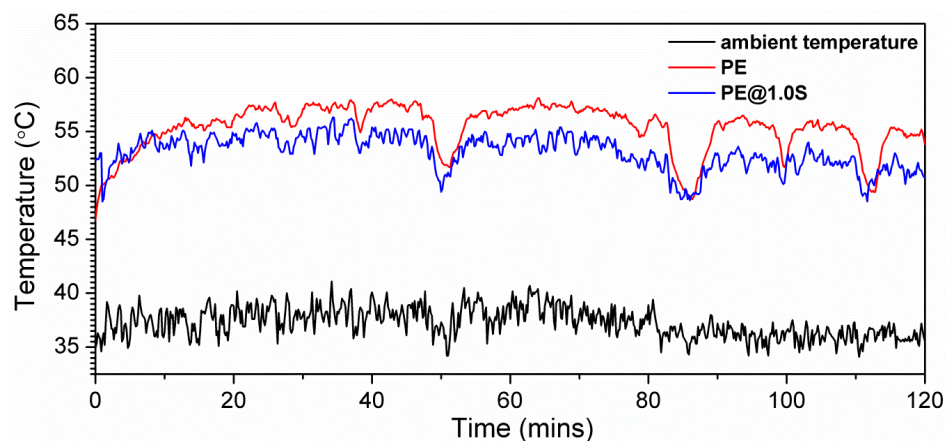


Figure 5. The temperature trend of PE and PE@1.0S inside the greenhouse, and the ambient temperature.

3.3. Energy Balance

The Earth's atmosphere has a transparency window in the infrared (IR) wavelength range between 8 and 13 μm and it can emit thermal radiation, which contributed to the radiative cooling. The most obvious difference in the spectra region between PE covering and the new greenhouse covering (PE@1.0S) was within 8–13 μm , i.e., the atmosphere window. In order to discuss the efficacy of the passive cooling, we observed and calculated the cooling heat power only for wavelengths of 8–13 μm . Therefore, we replaced the wavelength range of zero to infinite in each formula with 8×10^{-6} m to 13×10^{-6} m. When a greenhouse was facing clear sky, the net cooling power P_{net} of the surface was determined by the following:

$$P_{net}(T_s, T_a) = P_{rad}(T_s) - P_{atm}(T_a) - P_{solar} - P_c \quad (2)$$

where T_s is the surface temperature, T_a is the ambient temperature, P_{rad} is the thermal emission power radiated out by the substance, P_{atm} is the absorbed atmospheric irradiation at a temperature T_a , P_{solar} is the incident solar power absorbed by the structure, and P_c is the nonradiative (i.e., conductive + convective) heat transfer, and the thermal emission power radiated out by the film is as follows:

$$P_{rad}(T_s) = \int_0^{\pi/2} \int_{8e-6}^{13e-6} I_{bb}(T_s, \lambda) \varepsilon_s(\lambda, \theta) 2\pi \sin\theta \cos\theta d\lambda d\theta \quad (3)$$

Here, $I_{bb}(T, \lambda) = \frac{2hc^2}{\lambda^5 e^{hc/\lambda kT} - 1}$ is the spectral radiance of a black body, defined by Planck's law at any temperature, T (K), where h is Planck's constant 6.626×10^{-34} J·s $^{-1}$, k is the Boltzmann constant 1.3806×10^{-23} J·K $^{-1}$, c is the speed of light in a vacuum 3×10^8 m·s $^{-1}$, λ is the wavelength (m), T_s is the surface temperature of the film, and $\varepsilon_s(\lambda, \theta)$ is the emissivity of the surface as a function of wavelength and direction, which in this article, is not considered the function of direction in $\varepsilon_s(\lambda, \theta)$. We replaced the covering's emissivity with its absorptivity by using Kirchhoff's radiation law.

$$P_{atm}(T_a) = \int_0^{\pi/2} \int_{8e-6}^{13e-6} I_{bb}(T_a, \lambda) \varepsilon_s(\lambda, \theta) \varepsilon_a(\lambda, \theta) 2\pi \sin\theta \cos\theta d\lambda d\theta \quad (4)$$

$P_{atm}(T_a)$ is the absorbed atmospheric irradiation at a temperature T_a , and $\varepsilon_a(\lambda, \theta)$ is the emissivity of atmosphere as a function of direction and wavelength. The angle-dependent emissivity of the atmosphere between 8 and 13 μm is given by $\varepsilon_a(\lambda, \theta) = 1 - 0.87^{1/\cos\theta}$ [24], and T_a is the ambient temperature.

We integrated the FTIR spectrum (as shown in Figure 2) by using origin Pro8 in order to get the transmittance within 8 μm and 13 μm . For PE, the transmittance was 68.68%, and in the case of ignoring the reflection, the absorptivity was 0.3132, i.e., $\varepsilon_s(\lambda, \theta) = 0.3132$. According to Figure 4, the average temperature on the PE covering was 52.01 $^\circ\text{C}$, i.e., $T_s = 52.01 + 273 = 325.01$, the average ambient temperature was 37.28 $^\circ\text{C}$, i.e., $T_a = 37.28 + 273 = 310.28$, and $\varepsilon_a(\lambda, \theta) = 1 - 0.87^{1/\cos\theta}$, so $P_{rad}(\text{PE}) = 66.6931$ W m $^{-2}$ and $P_{atm}(\text{PE}) = 11.9890$ W m $^{-2}$ were calculated by MATLAB2017.

However, for PE@1.0S, the transmittance was 46.27%, and if ignoring the reflection, the absorptivity was 0.5373, i.e., $\varepsilon_s(\lambda, \theta) = 0.5373$. The average temperature on the new greenhouse covering was 49.69 $^\circ\text{C}$, i.e., $T_s = 49.69 + 273 = 322.69$, and the average ambient temperature was 37.28 $^\circ\text{C}$, i.e., $T_a = 37.28 + 273 = 310.28$, as shown in Figure 4, and $\varepsilon_a(\lambda, \theta) = 1 - 0.87^{1/\cos\theta}$; therefore, $P_{rad}(\text{PE@1.0S}) = 110.8249$ W m $^{-2}$ and $P_{atm}(\text{PE@1.0S}) = 20.5640$ W m $^{-2}$ were computed by MATLAB2017.

$$P_{solar} = \int_{8e-6}^{13e-6} I_{AM1.5}(\lambda) \varepsilon_s(\lambda, 0) d\lambda \quad (5)$$

P_{solar} is the incident solar absorption power by the films as in the following formula. To our knowledge, the spectral irradiance of AM1.5 is mainly concentrated on the wavelength between 0.3 μm

and 3 μm , and above 3 μm is almost close to zero. In this study, we only discussed the wavelength within the atmospheric window (8–13 μm). Therefore, whether it was for PE or PE@1.0S, P_{solar} was considered to be zero here, which was $P_{\text{solar}}(\text{PE}) = 0$ and $P_{\text{solar}}(\text{PE@1.0S}) = 0$.

$$P_C = h_c(T_a - T_s) \quad (6)$$

The last item in the formula, P_C , is the nonradiative heat transfer, where h_c ($\text{W}\cdot\text{m}^{-2}\cdot\text{K}^{-1}$) is the convection heat transfer coefficient, which is related to the wind speed. Generally, for applications above ambient temperature, nonradiative heat transfer is advantageous for the cooling process, but for applications below ambient temperature, nonradiative heat transfer is detrimental for the cooling process.

Because our experiments were carried out in a narrow space surrounded by buildings, and the wind was small, in this study, we only considered natural convective heat transfer. The natural convection coefficient was calculated using the method in the website “QuickField”. The greenhouse surfaces were divided into vertical plane and inclined plane and their natural convection coefficients were $3.5 \text{ W}\cdot\text{m}^{-2}\cdot\text{K}^{-1}$ and $3.3 \text{ W}\cdot\text{m}^{-2}\cdot\text{K}^{-1}$, respectively, and we took the $h_{\text{ave}} = 3.4 \text{ W}\cdot\text{m}^{-2}\cdot\text{K}^{-1}$ to perform further calculations. $P_C(\text{PE}) = 3.4 \times (310.28 - 325.01) = -50.082 \text{ W}\cdot\text{m}^{-2}$, and $P_C(\text{PE@1.0S}) = 3.4 \times (310.28 - 322.69) = -42.194 \text{ W}\cdot\text{m}^{-2}$. Finally, $P_{\text{net}}(\text{PE}) = 66.6931 - 11.9890 - (-50.082) = 104.7861 \text{ W}\cdot\text{m}^{-2}$, and $P_{\text{net}}(\text{PE@1.0S}) = 110.8249 - 20.5640 - (-42.194) = 132.4549 \text{ W}\cdot\text{m}^{-2}$, so the cooling effect of PE@1.0S is about $28 \text{ W}\cdot\text{m}^{-2}$ higher than that of PE. It implies that the addition of the nonmetal oxide particles could enhance the cooling performance of the greenhouse due to radiative cooling.

4. Conclusions

In this study, a new greenhouse covering (PE@1.0S) made of a PE–matrix composite was developed.

1. FTIR spectra displayed that an obvious absorption appeared near 1000 cm^{-1} due to nonmetal oxide particles, and a peak at 1575 cm^{-1} was attributed to the characteristic absorption of the conjugated C=N in the hindered amine light stabilizers;
2. Under ambient conditions of $35 \text{ }^\circ\text{C}$, the inner temperature of the simulated greenhouse with PE@1.0S was $2.2 \text{ }^\circ\text{C}$ less than that of the simulated greenhouse with the PE cladding. It is believed that the cooling performance of the greenhouse was due to passive radiative cooling;
3. Considering the natural convection heat transfer, under the environmental conditions of $35 \text{ }^\circ\text{C}$, the net cooling power of the greenhouse film developed in this study was $28 \text{ W}\cdot\text{m}^{-2}$ higher than that of the conventional PE film, due to passive radiative cooling;
4. With the increasingly severe energy states and environmental problems, radiative cooling is significant in reducing building energy consumption. Therefore, it is necessary to further study how to use radiant cooling to reduce the temperature of greenhouses to save energy.

Author Contributions: Conceptualization, M.-T.L.; methodology, M.-T.L.; validation, C.-H.L.; formal analysis, C.-H.L.; investigation, C.-H.L. and C.-Y.T.; resources, C.A.; data curation, C.-Y.T.; writing (original draft preparation), C.-H.L.; writing (review and editing), M.-T.L.; supervision, C.A.; project administration, M.-T.L.; funding acquisition, C.A.

Funding: This research was funded by Ministry of Education, Executive Yuan, Taiwan.

Acknowledgments: The Ministry of Education, Executive Yuan, Taiwan, is acknowledged for supporting this study.

Conflicts of Interest: The authors declare no conflict of interest.

References

1. Oropeza-Perez, I.; Østergaard, P.A. Active and passive cooling methods for dwellings: A review. *Renew. Sustain. Energy Rev.* **2018**, *82*, 531–544. [[CrossRef](#)]
2. Ascione, F. Energy conservation and renewable technologies for buildings to face the impact of the climate change and minimize the use of cooling. *Sol. Energy* **2017**, *154*, 34–100. [[CrossRef](#)]
3. Givoni, B. Solar heating and night radiation cooling by a roof radiation trap. *Energ. Build.* **1977**, *1*, 141–145. [[CrossRef](#)]
4. Harrison, A.; Walton, M. Radiative cooling of TiO₂ white paint. *Sol. Energy* **1978**, *20*, 185–188. [[CrossRef](#)]
5. Mihalakakou, G.; Ferrante, A.; Lewis, J. The cooling potential of a metallic nocturnal radiator. *Energy Build.* **1998**, *28*, 251–256. [[CrossRef](#)]
6. Granqvist, C.; Hjortsberg, A. Radiative cooling to low temperatures: General considerations and application to selectively emitting SiO films. *J. Appl. Phys.* **1981**, *52*, 4205–4220. [[CrossRef](#)]
7. Rephaeli, E.; Raman, A.; Fan, S. Ultrabroadband photonic structures to achieve high-performance daytime radiative cooling. *Nano Lett.* **2013**, *13*, 1457–1461. [[CrossRef](#)]
8. Samuel, D.L.; Nagendra, S.S.; Maiya, M. Passive alternatives to mechanical air conditioning of building: A review. *Build. Environ.* **2013**, *66*, 54–64. [[CrossRef](#)]
9. Zhu, L.; Raman, A.; Fan, S. Color-preserving daytime radiative cooling. *Appl. Phys. Lett.* **2013**, *103*, 223902. [[CrossRef](#)]
10. Raman, A.P.; Anoma, M.A.; Zhu, L.; Rephaeli, E.; Fan, S. Passive radiative cooling below ambient air temperature under direct sunlight. *Nature* **2014**, *515*, 540. [[CrossRef](#)]
11. Hossain, M.M.; Jia, B.; Gu, M. A metamaterial emitter for highly efficient radiative cooling. *Adv. Opt. Mater.* **2015**, *3*, 1047–1051. [[CrossRef](#)]
12. Zhai, Y.; Ma, Y.; David, S.N.; Zhao, D.; Lou, R.; Tan, G.; Yang, R.; Yin, X. Scalable-manufactured randomized glass-polymer hybrid metamaterial for daytime radiative cooling. *Science* **2017**, *355*, 1062–1066. [[CrossRef](#)]
13. Kou, J.-L.; Jurado, Z.; Chen, Z.; Fan, S.; Minnich, A.J. Daytime radiative cooling using near-black infrared emitters. *ACS Photonics* **2017**, *4*, 626–630. [[CrossRef](#)]
14. Hernández, D.; Garín, M.; Trifonov, T.; Rodríguez, A.; Alcubilla, R. Emissive properties of SiO₂ thin films through photonic windows. *Appl. Phys. Lett.* **2012**, *100*, 091901. [[CrossRef](#)]
15. Gentle, A.R.; Smith, G.B. Radiative heat pumping from the Earth using surface phonon resonant nanoparticles. *Nano Lett.* **2010**, *10*, 373–379. [[CrossRef](#)]
16. Zhu, L.; Raman, A.P.; Fan, S. Radiative cooling of solar absorbers using a visibly transparent photonic crystal thermal blackbody. *Proc. Natl. Acad. Sci. USA* **2015**, *112*, 12282–12287. [[CrossRef](#)]
17. Liu, C.-H.; Ay, C.; Kan, J.-C.; Lee, M.-T. The effect of radiative cooling on reducing the temperature of greenhouses. *Materials* **2018**, *11*, 1166. [[CrossRef](#)]
18. Hossain, M.; Gu, M. Radiative cooling: Principles, progress, and potentials. *Adv. Sci.* **2016**, *3*, 1500360. [[CrossRef](#)]
19. Smith, G.; Gentle, A. Radiative cooling: Energy savings from the sky. *Nat. Energy* **2017**, *2*, 17142. [[CrossRef](#)]
20. Zeyghami, M.; Goswami, D.Y.; Stefanakos, E. A review of clear sky radiative cooling developments and applications in renewable power systems and passive building cooling. *Sol. Energy Mater. Sol. Cells* **2018**, *178*, 115–128. [[CrossRef](#)]
21. Li, H.; Zhao, J.; Li, M.; Deng, S.; An, Q.; Wang, F. Performance analysis of passive cooling for photovoltaic modules and estimation of energy-saving potential. *Sol. Energy* **2019**, *181*, 70–82. [[CrossRef](#)]
22. Gentle, A.R.; Smith, G.B. A subambient open roof surface under the Mid-Summer sun. *Adv. Sci.* **2015**, *2*, 1500119. [[CrossRef](#)] [[PubMed](#)]
23. Lu, X.; Xu, P.; Wang, H.; Yang, T.; Hou, J. Cooling potential and applications prospects of passive radiative cooling in buildings: The current state-of-the-art. *Renew. Sustain. Energy Rev.* **2016**, *65*, 1079–1097. [[CrossRef](#)]
24. Aili, A.; Zhao, D.; Lu, J.; Zhai, Y.; Yin, X.; Tan, G.; Yang, R. A kW-scale, 24-hour continuously operational, radiative sky cooling system: Experimental demonstration and predictive modeling. *Energy Convers. Manag.* **2019**, *186*, 586–596. [[CrossRef](#)]
25. Zhao, D.; Aili, A.; Zhai, Y.; Lu, J.; Kidd, D.; Tan, G.; Yin, X.; Yang, R. Subambient cooling of water: Toward real-world applications of daytime radiative cooling. *Joule* **2019**, *3*, 111–123. [[CrossRef](#)]

26. Zhao, D.; Aili, A.; Zhai, Y.; Xu, S.; Tan, G.; Yin, X.; Yang, R. Radiative sky cooling: Fundamental principles, materials, and applications. *Appl. Phys. Rev.* **2019**, *6*, 021306. [[CrossRef](#)]
27. Wang, S.; Zhang, J.; Liu, L.; Yang, F.; Zhang, Y. Evaluation of cooling property of high density polyethylene (HDPE)/titanium dioxide (TiO₂) composites after accelerated ultraviolet (UV) irradiation. *Sol. Energy Mater. Sol. Cells* **2015**, *143*, 120–127. [[CrossRef](#)]
28. Abdel-Ghany, A.M.; Al-Helal, I.M.; Alzahrani, S.M.; Alsadon, A.A.; Ali, I.M.; Elleithy, R.M. Covering materials incorporating radiation-preventing techniques to meet greenhouse cooling challenges in arid regions: A review. *Sci. World J.* **2012**, *2012*, 906360. [[CrossRef](#)]
29. Abdel-Ghany, A.M.; Kozai, T.; Kubota, C.; Taha, I.S. Investigation of the spectral optical properties of the liquid radiation filters for using in the greenhouse applications. *J. Agric. Meteorol.* **2001**, *57*, 11–19. [[CrossRef](#)]
30. Adam, A.; Kouider, S.; Youssef, B.; Hamou, A.; Saiter, J. Studies of polyethylene multi layer films used as greenhouse covers under Saharan climatic conditions. *Polym. Test.* **2005**, *24*, 834–838. [[CrossRef](#)]
31. Baille, A.; Kittas, C.; Katsoulas, N. Influence of whitening on greenhouse microclimate and crop energy partitioning. *Agric. For. Meteorol.* **2001**, *107*, 293–306. [[CrossRef](#)]
32. Edser, C. Light manipulating additives extend opportunities for agricultural plastic films. *Plast. Addit. Compd.* **2002**, *4*, 20–24. [[CrossRef](#)]
33. Gulrez, S.K.; Abdel-Ghany, A.M.; Al-Helal, I.M.; Al-Zaharani, S.M.; Alsadon, A.A. Evaluation of PE films having NIR-reflective additives for greenhouse applications in arid regions. *Adv. Mater. Sci. Eng.* **2013**, *2013*, 8. [[CrossRef](#)]
34. Hemming, S.; Kempkes, F.; Van der Braak, N.; Dueck, T.; Marissen, N. Greenhouse cooling by NIR-reflection. *Int. Symp. Greenh. Cool.* **2006**, *719*, 97–106.
35. Hoffmann, S.; Waaijenberg, D. Tropical and subtropical greenhouses—A challenge for new plastic films. *Int. Symp. Des. Environ. Control Trop. Subtrop. Greenh.* **2001**, *578*, 163–169. [[CrossRef](#)]
36. Jeevanandam, P.; Mulukutla, R.; Phillips, M.; Chaudhuri, S.; Erickson, L.; Klabunde, K. Near infrared reflectance properties of metal oxide nanoparticles. *J. Phys. Chem. C* **2007**, *111*, 1912–1918. [[CrossRef](#)]
37. Markarian, J. Plasticulture comes of age. *Plast. Addit. Compd.* **2005**, *7*, 16–19. [[CrossRef](#)]
38. Revel, G.M.; Martarelli, M.; Bengochea, M.Á.; Gozalbo, A.; Orts, M.J.; Gaki, A.; Gregou, M.; Taxiarchou, M.; Bianchin, A.; Emiliani, M. Nanobased coatings with improved NIR reflecting properties for building envelope materials: Development and natural aging effect measurement. *Cem. Concr. Comp.* **2013**, *36*, 128–135. [[CrossRef](#)]



© 2019 by the authors. Licensee MDPI, Basel, Switzerland. This article is an open access article distributed under the terms and conditions of the Creative Commons Attribution (CC BY) license (<http://creativecommons.org/licenses/by/4.0/>).